

# Structural and Dynamical Features of Multiple Metastable Glassy States in a Colloidal System with Competing Interactions

Christian L. Klix,<sup>1,2</sup> C. Patrick Royall,<sup>1,3</sup> and Hajime Tanaka<sup>1</sup>

<sup>1</sup>*Institute of Industrial Science, University of Tokyo, Meguro-ku, Tokyo 153-8505, Japan*

<sup>2</sup>*University of Konstanz, 78457 Konstanz, Germany*

<sup>3</sup>*School of Chemistry, University of Bristol, Bristol BS8 1TS, United Kingdom*

(Received 24 September 2009; published 23 April 2010)

Systems in which a short-ranged attraction and long-ranged repulsion compete are intrinsically frustrated, leading their structure and dynamics to be dominated either by mesoscopic order or by metastable disorder. Here, we report the latter case in a colloidal system with long-ranged electrostatic repulsions and short-ranged depletion attractions. We find a variety of states exhibiting slow nondiffusive dynamics: a gel, a glassy state of clusters, and a state reminiscent of a Wigner glass. Varying the interactions, we find a continuous crossover between the Wigner and cluster glassy states, and a sharp discontinuous transition between the Wigner glassy state and gel. Our results suggest that a balance between repulsions and attractions controls the nature of dynamic arrest of these glassy states.

DOI: 10.1103/PhysRevLett.104.165702

PACS numbers: 64.70.pv, 64.60.My, 64.70.kj, 82.70.Gg

In general, attractive interactions promote ordered phases or condensates, whereas long-ranged repulsions inhibit this tendency, fundamentally redefining the free energy leading to complex phases that break translational and/or rotational symmetry. Such mesoscopic ordering occurs in a diverse range of materials [1,2], from the pasta phase in neutron stars [3], highly correlated quantum Hall and strongly correlated electron systems such as high  $T_c$  superconductors [2,4] to classical systems [1] such as ferromagnetic films, diblock copolymers, colloids [5,6], and biological systems. It has been suggested [5–8] that competing interactions cause frustration, leading to exotic nonergodic disordered states. In the above examples, the system can relax locally; it is rather rare to see metastable disorder at the local level. Locally disordered states were however reported for suspensions of Laponite clay particles, but the anisotropic particles and interactions make the situation rather complex [9].

Hard spheres with an attraction provide a model which captures the essence of atoms and small molecules. Short-ranged attractions lead to gelation due to arrested phase separation [10]. At higher densities, both hard-sphere and attractive glasses are found [Fig. 1(g)] [11], along with gels [12]. Long-range repulsions can lead to glasses at low densities [13,14], and combined with short-ranged attractions, the behavior is very rich. Indeed, many properties of biological materials may be connected to competing interactions [15]. For example, globular proteins are rather well described as spheres with short-ranged attractions and long-ranged repulsions [16]. While most biological systems are more complex, it is important to understand this seemingly simple addition to well-studied models of atoms, not least as it offers insight into transitions between metastable states.

Since competing interactions lead to frustration between phase separation and homogeneity, a characteristic length

scale is often predicted from computer simulation, for example, periodic lamellae [6] or low-dimensional clusters of a specific size [17]. These may then undergo hierarchical self-organization; in particular, clusters may themselves be implicated in gelation [18] and undergo dynamical arrest to form a “cluster glass” [19]. Despite recent developments [16,20,21], experimental work in colloidal systems with competing interactions has so far found

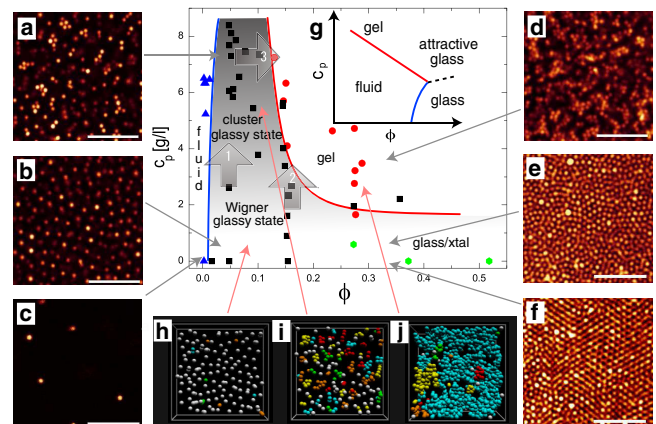


FIG. 1 (color online). State diagram of our system and 2D structures: (a) cluster glassy ( $\phi = 0.04$ ,  $c_p = 8.39$  g/l), (b) Wigner glassy (0.047, 0), (c) fluid (0.002, 0), (d) gel (0.152, 4.10), (e) Wigner glassy (0.372, 0), and (f) crystal (0.372, 0) state. Bars are  $20 \mu\text{m}$ . Increasing grey shading represents increasing amount of clusters. Thick arrows denote paths 1–3 described in the text. Glassy state is denoted by squares, gel by circles, crystal or glassy state by hexagons and fluid by triangles. (g) State diagram of a system without long-ranged repulsions [11], showing two glassy states at high  $\phi$ . (h)–(j): 3D structures of (h) Wigner glassy, (i) cluster glassy, and (j) gel state. White particles have no neighbors, otherwise colors denote connected regions. Images represent characteristic (seemingly stationary) structures of the system at  $t > \sim 10\tau$  after homogenization.

little evidence of periodic structures, although gels with novel structures [20,21] and low-dimensional clusters [20,22] have been seen.

We consider spherical colloids (diameter  $\sigma$ ) immersed in a solvent, with a relatively strong, long-range electrostatic repulsion, and a short-range, tunable attraction mediated by nonadsorbing polymer whose strength is set by the polymer concentration  $c_p$ , and range by polymer size, here the polymer-colloid size ratio  $q \sim 0.19$  (see supplementary information [23]). We determined the magnitude of the electrostatic repulsions from fitting the structure of equilibrium fluids [24,25] which gave a colloid charge number of  $Z \sim 600 \pm 200$  (see [26,23]). According to mode-coupling theory [29], for our parameters, we expect a transition to a Wigner glass at comparable colloid volume fractions to those observed experimentally. Mixing the samples prior to imaging leads to a randomized state, after which the tuned interactions and colloid volume fraction  $\phi$  yield a (metastable) point on the state diagram (Fig. 1). The waiting time prior to imaging was always greater than  $10\tau$  ( $\tau$ : the characteristic particle diffusion time, see [23]). We sometimes see the formation of a Wigner crystal state at  $\phi > 0.2$  and low  $c_p$ ; however, this is a rare event [see Fig. 1(f)], usually the system forms a glassy state before crystallization [23]. Using real space structural and dynamical analysis, we find a state diagram dominated by three glassy states with different disordered structures: Wigner glassy state, cluster glassy state, and gel. We study the transitions between these states and reveal their nature.

We begin by presenting the state diagram in Fig. 1, which underlines the extent to which the system is dominated by dynamically arrested states. A low-density colloidal fluid ( $\phi = 0.002$ ) where the system is ergodic is shown in Fig. 1(c). Increasing the volume fraction to  $\phi = 0.016$  results in a glassy state where the slow dynamics is driven by the long-ranged electrostatic repulsions [Figs. 1(b), 1(e), and 1(h)]. We thus term this state a “Wigner glassy state.” At low  $\phi$  and higher  $c_p$ , we see the formation of clusters and term this state a “cluster glassy state” [Figs. 1(a) and 1(i)]. Meanwhile, increasing both  $c_p$  and  $\phi$  results in a gel which we define through percolation [Figs. 1(d) and 1(j)], and appears dynamically arrested [Fig. 2(a)]. A schematic state diagram for a colloidal system without electrostatic repulsions is shown in Fig. 1(g). We see striking differences in the structure of the state diagram between systems with and without electrostatic repulsions (see also [23]). Without electrostatic repulsions, slow dynamics occur at a higher absolute volume fraction than we observe; however, because of the long-ranged repulsions, the effective size of the colloids is increased, so we compare our low-density system with hard spheres at higher  $\phi$ . With electrostatics the ergodic region is very narrow, around  $\phi \sim 0$ , and the glassy states dominate the state diagram.

Before discussing the structure of these three states in more detail, let us consider the dynamics. Mean squared

displacement (MSD) measurements, in which the colloids are tracked in two dimensions (2D), are shown in Fig. 2. The (ergodic) fluid we see at low  $\phi$  appears to exhibit diffusive behavior, and the gel appears dynamically arrested, within the accuracy to which we can track the particles (100 nm or  $\sigma/20$ ). The other states show extensive nondiffusive behavior, yet they do not reach a clear plateau on the experimental time scale although we track the particles for up to  $72\tau$  (20 hours) for the cluster glassy state and up to  $40\tau$  for the Wigner glassy state. At long times, particle tracking is limited by tracking errors, residual sedimentation, bleaching, and drift. We estimate the cage size as the width of the first and second peaks in  $g(r)$  for the Wigner and cluster glassy states, respectively [see Fig. 3(a)]. For the gel, the cage size is taken as the bond length,  $0.19\sigma$ . Concerning the cluster glassy state, similar subdiffusive behavior has recently been seen in simulation [19]. We note that such behavior is expected because clusters can rotate as rigid bodies [see Fig. 2(b)]. This strong decoupling between translational and rotational motion may be unique to a cluster glassy state. In the case of the Wigner glassy state, based upon simulation work in a similar system [30], we believe that our experimental time scales limit full access to relaxation phenomena. In any case, the cage size is not reached [see Fig. 2(a)]. The soft nature of the interactions also prolongs the subdiffusive regime and makes a rigorous confirmation of nonergodicity very challenging. The nondiffusive behavior is suggestive of the glassiness of these states. Since we do not find a clear plateau experimentally, we term these “cluster glassy state” and “Wigner glassy state,” respectively, although these may be practically regarded as nonergodic.

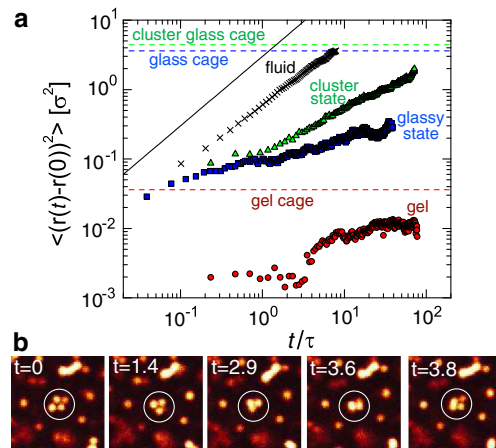


FIG. 2 (color online). (a) Mean square displacements. Crosses = fluid ( $\phi = 0.002$ ,  $c_p = 0$  g/l), green triangles = cluster glassy state (0.051, 5.16), red circles = gel (0.275, 4.88), and blue squares = glassy state (0.069, 0). Dashed lines corresponding to the cage size are plotted for gel ( $0.19\sigma$ ), Wigner state ( $1.9\sigma$ ) and cluster state ( $2.1\sigma$ ), respectively. (b) A cluster spinning process in its “cage” (see movie 1 [23]). Time unit =  $\tau$ , image width =  $19.5 \mu\text{m}$ .

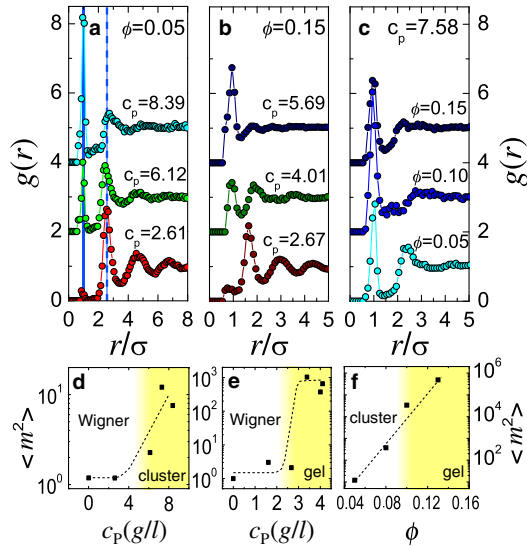


FIG. 3 (color online). (a) (path 1) shows the change in  $g(r)$  across the Wigner-cluster glassy state transition. Vertical solid line indicates the peak at contact ( $r = \sigma$ ), and dashed line indicates the first peak of  $g(r)$  of the Wigner glassy state, corresponding to the average interparticle distance, and the second peak of  $g(r)$  of the cluster glassy state, corresponding to the first shell of clusters. (b) (path 2) from a Wigner glassy to a gel state, and (c) (path 3) from a cluster glassy to a gel state.  $c_p$  is given in units of g/l. Data offset for clarity. (d) The change in  $\langle m^2 \rangle$  along path 1 (at  $\phi = 0.051$ ), (e) along path 2 (at  $\phi = 0.151$ ), and along (f) path 3 (at  $c_p = 7.58$  g/l). Dashed lines and shading are guides to the eye.

The state diagram dominated by these three glassy states illustrated in Fig. 1 yields three transitions. It is a commonly held view that dynamical arrest is accompanied by little structural change. While literature on transitions between glassy states is scarce, the structural change in the attractive-repulsive glass transition at high  $\phi$  is rather subtle [31]. Conversely, all states identified here are characterized by structure [see Figs. 1(h)–1(j)]. We show a considerable variety of metastable structures in the response to small changes in parameters.

Let us now enquire as to the nature of the transitions between these glassy states. The transition between Wigner and cluster glassy states (path 1 in Fig. 1) is shown in Figs. 3(a) and 3(d), the radial distribution function  $g(r)$  and the variance in the cluster size distribution  $\langle m^2 \rangle$ , where  $m$  is the number of particles per cluster. Rather than a sharp transition, the Wigner glassy state is unaffected by weak attractions; until the polymer concentration exceeds around  $c_p = 4$  g/l, there is no response in the size distribution. At higher  $c_p$ , there is an increase in (cluster) size, yet our data suggest that it occurs rather gradually; i.e., passing from the Wigner to the cluster glassy state is a crossover rather than a sharp transition: particles start to form small clusters above a certain threshold  $c_p$ , and their size gradually increases with an increase in  $c_p$ . The gradual development of the peak at contact (at  $r = \sigma$ ) in the  $g(r)$

[Fig. 3(a)] further supports this observation. Note that the emergence of the peak at contact is a direct consequence of attractions. In equilibrium, the repulsive Wigner state (comprised of monomers) is expected to be a crystal. The same can apply to states of *monodisperse* clusters [32]; however, here the clusters are very polydisperse (see Fig. 1(a) and [23]), causing self-generated disorder, intrinsically suppressing crystallization. This disorder is a consequence of a two-level hierarchy, of colloids forming clusters and then clusters forming a glass which may be characteristic of a system of competing interactions with different ranges.

Proceeding to the transition between the Wigner glassy and gel states (path 2 in Fig. 1), we find a rather different scenario. Raising the colloid volume fraction to  $\phi = 0.15$ , the  $g(r)$  [Fig. 3(b)] again shows the development of a peak at contact ( $r = \sigma$ ) around  $c_p = 4$  g/l. We recall that at lower  $\phi$ , at a similar  $c_p$ , clusters began to form [Fig. 3(a)]. For  $\phi = 0.15$ , this yields percolation [Fig. 1(j)], and a sharp transition to a gel state [Fig. 3(e)], accompanying a strong increase in  $\langle m^2 \rangle$  by about 3 orders of magnitude. This is markedly different from the continuous increase in  $\langle m^2 \rangle$  for the Wigner-cluster glassy states [see Fig. 3(d)].

What happens in the case of the transition between cluster glassy and gel states? Path 3 in Fig. 1 is shown in Figs. 3(c) and 3(f). Unlike the previous transitions, here the polymer concentration is fixed at  $c_p = 7.4$  g/l. In fact, rather little change in local structure is seen in the  $g(r)$  analysis [Fig. 3(c)], and the variance in the cluster size increases continuously. Our results indicate that, in contrast to paths 1 and 2 in Fig. 1, the cluster glass-gel boundary is delineated by a percolation transition, rather than by local structural changes.

We also observed a novel aging mechanism in the cluster state. While aging is usually thought of in dynamic terms, here we present a structural mechanism. This concerns the transition from a state of high potential energy, a cluster of charged particles, to a smaller cluster, via cluster fission. We never observed any cluster fusion, and particle tracking shows a continuous rise in the population of small clusters as a function of time. The emission process occurs in less than 1/100 of the characteristic diffusion time, a much faster time scale than structural relaxation even in the absence of slow dynamics. This phenomenon is illustrated in Figs. 4(a) and 4(b). This cluster state suffers from a complex minimization problem involving the spatial distributions of colloids, counterions, and polymers. The coupling between these quantities yields a complex energy landscape. This fission process allows us to directly observe a kinetic path from one local minimum to a neighboring minimum with a lower energy. For details, see [23].

In closing, we found that the introduction of relatively strong, long-ranged repulsions to a colloidal dispersion with short-range attractions generates novel glassy states, such as the cluster glassy state, and drastically transforms behavior, at that most fundamental of levels: the ability of

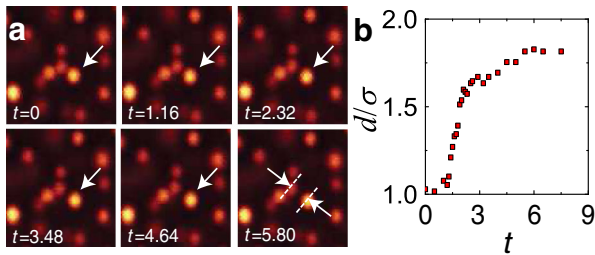


FIG. 4 (color online). Aging mechanism of a cluster glassy state. (a) An emission process from an  $m = 5$  to  $m = 4$  cluster, as shown by arrows (see movie 2 [23]) at  $\phi = 0.051$  and  $c_p = 5.158$  g/l. Time  $t$  is expressed in units of  $\tau/1000$ , and the image width is  $14 \mu\text{m}$ . (b) Separation of the emitted particle and cluster, as defined by arrows in (a), as a function of  $t$ .

the system to relax locally. For a system of short-ranged attractive interactions, one may distinguish the repulsive hard-sphere glass and the attractive glass, as depicted in Fig. 1(g) [11], but there the change in the structure is rather subtle [31]. In contrast, the transitions between cluster glassy and gel states and between Wigner glassy and gel states both accompany significant structural changes from single particle to compact clusters and a percolating network, respectively. The observed behavior can be interpreted as the interplay of a Wigner glassy state dominated by long-range repulsions with formation of clusters driven by short-range attractions [17] and their percolation leading to gelation. The primary driver of arrest for gel may continuously change from repulsions to attractions with an increase in  $\phi$  (see [23]). The existence of such multiple glassy states is reminiscent of Laponite [9]; however, some differences in the state diagram may arise from the fact that in Laponite, the repulsion is controlled by salt, but here, the attraction is controlled by polymers. For example, the gel region does not share any boundary with an ergodic liquid state in our case. The effect of long-ranged repulsions on the state diagram of a system with short-ranged attractions is an interesting fundamental problem; at intermediate repulsions, a cluster fluid emerges [20–22]. Since protein solutions also exhibit comparable interactions, it may be reasonable to suppose equilibrium cluster phases [16,33] and perhaps even cluster glasses.

The authors are grateful to Didi Derks, Rob Jack, and Matthias Schmidt for a critical reading of the manuscript. C.L.K. thanks the Deutscher Akademischer Austauschdienst for financial assistance. C.P.R. acknowledges the Royal Society for financial support. H.T. acknowledges a Grant-in-Aid from the Ministry of Education, Culture, Sports, Science and Technology, Japan.

- [1] M. Seul and D. Andelman, *Science* **267**, 476 (1995).  
[2] E. Dagotto, *Science* **309**, 257 (2005).

- [3] C.J. Horowitz *et al.*, *Phys. Rev. C* **69**, 045804 (2004).  
[4] V. Emery and S. Kivelson, *Physica C (Amsterdam)* **209**, 597 (1993).  
[5] F. Sciortino and P. Tartaglia, *Adv. Phys.* **54**, 471 (2005).  
[6] M. Tarzia and A. Coniglio, *Phys. Rev. Lett.* **96**, 075702 (2006).  
[7] F. Sciortino *et al.*, *Phys. Rev. Lett.* **93**, 055701 (2004).  
[8] G. Tarjus *et al.*, *J. Phys. Condens. Matter* **17**, R1143 (2005).  
[9] H. Tanaka, J. Meunier, and D. Bonn, *Phys. Rev. E* **69**, 031404 (2004).  
[10] P.J. Lu *et al.*, *Nature (London)* **453**, 499 (2008).  
[11] K.N. Pham *et al.*, *Science* **296**, 104 (2002).  
[12] Y. Gao and M.L. Kilfoil, *Phys. Rev. Lett.* **99**, 078301 (2007).  
[13] E.B. Sirota *et al.*, *Phys. Rev. Lett.* **62**, 1524 (1989).  
[14] E. Zaccarelli, *J. Phys. Condens. Matter* **19**, 323101 (2007).  
[15] C. Semmrich *et al.*, *Proc. Natl. Acad. Sci. U.S.A.* **104**, 20199 (2007).  
[16] A. Stradner *et al.*, *Nature (London)* **432**, 492 (2004).  
[17] J. Groenewold and W. Kegel, *J. Phys. Chem. B* **105**, 11702 (2001).  
[18] K. Kroy, M.E. Cates, and W.C.K. Poon, *Phys. Rev. Lett.* **92**, 148302 (2004).  
[19] J.C. Fernandez Toledano, F. Sciortino, and E. Zaccarelli, *Soft Matter* **5**, 2390 (2009).  
[20] A.I. Campbell, V.J. Anderson, J.S. van Duijneveldt, and P. Bartlett, *Phys. Rev. Lett.* **94**, 208301 (2005).  
[21] C.J. Dibble, M. Kogan, and M.J. Solomon, *Phys. Rev. E* **74**, 041403 (2006).  
[22] H. Sedgwick, S. Egelhaaf, and W.C.K. Poon, *J. Phys. Condens. Matter* **16**, S4913 (2004).  
[23] See supplementary material at <http://link.aps.org/supplemental/10.1103/PhysRevLett.104.165702> for supplementary information and movies 1 and 2.  
[24] C.P. Royall, A.A. Louis, and H. Tanaka, *J. Chem. Phys.* **127**, 044507 (2007).  
[25] C.P. Royall *et al.*, *J. Chem. Phys.* **124**, 244706 (2006).  
[26] Here, we note that a potential at contact is estimated as several hundred  $k_B T$ , substantially in excess of the attractive forces mediated by the depletion attraction,  $\sim 15k_B T$  for  $c_p = 2$  g/l at which we find clustering and gelation (see [23]) (note that for a charge-free system, gelation typically occurs with an attractive potential of  $\sim 3k_B T$ ). We believe that the charge is associated with the free surfaces of the colloids, and that clusters may have a markedly lower charge per colloid than do the isolated particles [27]. Calculations show that for such anisotropic charge distributions, the electrostatic repulsion is much reduced, enabling the clustering and gelation we observe [28].  
[27] C.L. Klix *et al.*, [arXiv:0905.3393](https://arxiv.org/abs/0905.3393).  
[28] N. Hoffman, C.N. Likos, and J.P. Hansen, *Mol. Phys.* **102**, 857 (2004).  
[29] S.K. Lai *et al.*, *Phys. Rev. E* **56**, 766 (1997).  
[30] E. Zaccarelli *et al.*, *Phys. Rev. Lett.* **100**, 195701 (2008).  
[31] N. Simeonova *et al.*, *Phys. Rev. E* **73**, 041401 (2006).  
[32] B.M. Mladek *et al.*, *Phys. Rev. Lett.* **96**, 045701 (2006).  
[33] A. Shukla *et al.*, *Proc. Natl. Acad. Sci. U.S.A.* **105**, 5075 (2008).